

Four-wave mixing between a soliton and noise in a system with large amplifier spacing

Sien Chi and Chuan-Yuan Kao

Institute of Electro-Optical Engineering, National Chiao Tung University, Hsinchu 30050, Taiwan, China

Senfar Wen

Department of Electrical Engineering, Chung-Hua Polytechnic Institute, Hsinchu 30067, Taiwan, China

Received June 3, 1997

Depletion of soliton energy by four-wave mixing between a soliton and amplifier noise in a system with 100-km amplifier spacing is studied. Dispersion exponentially decreasing fiber is used as transmission fiber. Improvement of the system by the use of a sliding-frequency filter to reduce noise power and the depletion of soliton energy is shown. The system can be further improved by compensation for depleted soliton energy.
© 1997 Optical Society of America

The amplifier spacing of a soliton-transmission system is limited by soliton stability and noise-induced timing jitter.^{1,2} These limits require that the amplifier spacing be much shorter than the soliton period to maintain stable soliton transmission. For large amplifier spacing the noise power introduced by the optical amplifier is significant. Therefore amplifier spacing shorter than ~50 km is usually used in a soliton system. For undersea optical cable systems, larger amplifier spacing is desirable. In this Letter we consider a soliton system with 100-km amplifier spacing, in which dispersion exponentially decreasing fiber³ (DEDF) is used as the transmission medium and a Fabry-Perot filter (FPF) is used as the in-line filter to reduce timing jitter.⁴ As a fundamental soliton is maintained along the DEDF, the stability condition is satisfied by use of DEDF. The in-line filter stabilizes the carrier frequency of the soliton and reduces timing jitter. It was found that there is significant four-wave mixing (FWM) between soliton and amplifier noise in such a system because of high noise power and phase matching. The soliton-noise FWM depletes the soliton energy, and the soliton broadens. The improvement of the system by the use of a sliding-frequency filter⁵ (SFF) to reduce noise power and the depletion of soliton energy is considered. In addition, the system can be further improved by compensation for the depleted soliton energy.

The pulse propagation in a DEDF can be described by the modified nonlinear Schrödinger equation

$$i \frac{\partial U}{\partial z} - \frac{1}{2} \beta_2(z) \frac{\partial^2 U}{\partial \tau^2} - i \frac{1}{6} \beta_3 \frac{\partial^3 U}{\partial \tau^3} + \gamma |U|^2 U = -\frac{1}{2} i \alpha U. \quad (1)$$

In Eq. (1), U is the normalized field envelope; $\beta_2(z) = \exp(-\alpha z)\beta_2(0)$ is the second-order dispersion, where $\beta_2(0)$ is the initial value at every amplification stage; β_3 is the third-order dispersion; $\gamma = n_2 \omega_0 / c A_{\text{eff}}$, where n_2 is the Kerr coefficient, ω_0 is the carrier frequency, c is the velocity of the light in vacuum, and A_{eff} is

the effective fiber cross section; α is the fiber loss. For the numerical calculations, the carrier wavelength is taken to be 1.55 μm and the other parameters are taken to be $\beta_3 = 0.14 \text{ ps}^3/\text{km}$, $n_2 = 3.2 \times 10^{-20} \text{ m}^2/\text{W}$, $A_{\text{eff}} = 50 \mu\text{m}^2$, and $\alpha = 0.2 \text{ dB/km}$. A FPF is inserted after every amplifier. We choose the bandwidth of the filter to be $\Delta\nu_f = 10\Delta\nu_s$, where the soliton spectral width is $\Delta\nu_s = 0.314/\tau_w$ and τ_w is the soliton pulse width (FWHM). We take $\tau_w = 10 \text{ ps}$ and $\tau_w = 20 \text{ ps}$ as examples to show the results.

Figure 1 shows the input 10-ps soliton and the pulse shape of the soliton after propagating 10,000 km along the DEDF with $\beta_2(0) = -0.5 \text{ ps}^2/\text{km}$, where the gain of every amplifier is $\exp(\alpha L_a)$ and the amplifier spacing is $L_a = 100 \text{ km}$. The spontaneous-emission factor of the amplifier is $n_{\text{sp}} = 1.2$. An in-line filter of 314-GHz bandwidth is used. The pulse shape of the soliton after propagating 10,000 km without amplifier noise being considered is also shown for comparison. One can see that soliton energy is significantly depleted by the interaction with amplifier noise. The

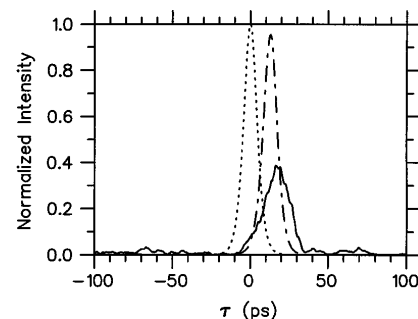


Fig. 1. Pulse shape of a 10-ps soliton after propagating 10,000 km along DEDF with $\beta_2(0) = -0.5 \text{ ps}^2/\text{km}$ (solid curve). The amplifier spacing is 100 km. An in-line filter with a 314-GHz bandwidth is used. The pulse shape of the input soliton is shown by the dotted curve. The pulse shape of the soliton after propagating 10,000 km without amplifier noise being considered is shown by the dashed-dotted curve.

interaction is due to the FWM between soliton and noise. The soliton-noise FWM is efficient because the noise power is high and the fiber dispersion is low in the considered DEDF. The asymmetric distortion of pulse shape is due mainly to the third-order fiber dispersion and the dispersion introduced by in-line filters. To estimate the soliton energy, we first filter the soliton with an ideal bandpass filter of bandwidth $\Delta\nu_w = 4\Delta\nu_s$. Then the soliton energy is calculated within a window of $\Delta\tau_w = 4\Delta\tau_s$ in the time domain, and the calculated energy is denoted as E_s . We simulate the transmission of a single soliton 16 times to obtain the average value of the soliton energy, \bar{E}_s . The ratio of the energy depletion is defined as

$$r_d = 1 - \bar{E}_s/E_{s0}, \quad (2)$$

where E_{s0} is the initial value of the soliton energy. Figure 2 shows the energy-depletion ratio r_d along the fiber for the case shown in Fig. 1. The ratio $r_n = E_n/E_{s0}$ is also shown in Fig. 2, where $E_n = n_{sp}(G - 1)\hbar\nu\Delta\nu_w\Delta\tau_w z/L_a$ is the accumulated noise energy without nonlinear mixing and z is the transmission distance. One can see that the noise energy from the optical amplifiers is small compared with the soliton energy, but the depletion of soliton energy owing to soliton-noise FWM is significant. From Fig. 2 one can see that r_d increases almost linearly with distance. At the end of 10,000-km transmission, \bar{E}_s is only two thirds of E_{s0} . The energy depletion manifests the pulse distortion shown in Fig. 1.

Figure 3 shows the depletion ratio r_d with respect to $|\beta_2(0)|$ for 10- and 20-ps solitons after the 10,000-km transmission distance. One can see that r_d can be reduced by the use of higher fiber dispersion. FWM is efficient when the soliton spectrum is near zero-dispersion frequency. The deviation of the zero-dispersion frequency from the carrier frequency of the soliton is $|\beta_2(z)|/\beta_3$. Within an amplifier spacing, as $|\beta_2(z)|$ decreases with distance the zero-dispersion frequency moves toward the soliton frequency. Therefore soliton-noise FWM increases with distance within an amplifier spacing. The smallest fiber dispersion is $|\beta_2(L_a)|$ at the end of every amplifier stage, and the zero-dispersion frequency lies within the soliton spectral width when $|\beta_2(L_a)| \leq \beta_3\pi\Delta\nu_s$. Thus the corresponding initial fiber dispersion $|\beta_2(0)|_{\min}$ can be estimated as a lower limit:

$$|\beta_2(0)|_{\min} = 0.314\pi\beta_3 \exp(\alpha L_a)/\tau_w, \quad (3)$$

where $|\beta_2(0)|_{\min} = 1.38 \text{ ps}^2/\text{km}$ and $|\beta_2(0)|_{\min} = 0.7 \text{ ps}^2/\text{km}$ for $\tau_w = 10 \text{ ps}$ and $\tau_w = 20 \text{ ps}$, respectively. Both of the depletion-ratio curves in Fig. 3 are almost linear for $|\beta_2(0)|$ above the lower-limit values, and the slopes increase drastically for $|\beta_2(0)|$ below them. Although a larger $|\beta_2(0)|$ leads to higher soliton power, the phase-matching condition is less well satisfied, and the efficiency of the soliton-noise FWM decreases in the case of the same pulse width. For the same $|\beta_2(0)|$, the r_d of the 10-ps soliton is smaller than the r_d of the 20-ps soliton since the former has a larger signal-to-noise ratio. If the pulse width is too short, the other effects such as third-order dispersion and self-frequency shift may deteriorate the pulse shape.

From Fig. 3, we can see that r_d decreases as $|\beta_2(0)|$ increases and the pulse width decreases. However, in the presence of neighboring solitons, and when noise-induced timing jitters are considered, the system performance may not be improved as $|\beta_2(0)|$ increases and the pulse width decreases.

To study the performance of the system, we considered the allowed transmission distance of a 10-Gbit/s system for a 10^{-9} bit-error rate. We simulated 254 bits to calculate the bit-error rate, where the probabilities of 1 and 0 bits were the same. The squares in Figs. 4(a) and 4(b) show the allowed transmission distances versus $|\beta_2(0)|$ for 10-ps and 20-ps solitons, respectively. It is known that the SFF can effectively reduce noise power and timing jitter.⁵ Soliton-noise FWM can also be reduced by use of a SFF. The crosses in Figs. 4(a) and 4(b) show the cases in which the SFF was used, where the filter is the same as the Fabry-Perot in-line filter used above except that the SFF's central frequency is upsliding, with rates of 3 and 5 GHz/Mm in Figs. 4(a) and 4(b), respectively. One can see that the improvement of the transmission distance ranges from 1000 to 2000 km and that there exists an optimum $|\beta_2(0)|$ for the maximum transmission distance. When $|\beta_2(0)|$ is small, soliton-noise FWM is significant. When $|\beta_2(0)|$ is large, although the energy-depletion ratio is reduced, as shown in Fig. 3, soliton-soliton interaction and noise-induced timing jitter are enhanced and the transmission distance is limited. Comparing Figs. 4(a) and 4(b) shows that, for $|\beta_2(0)| < 0.6 \text{ ps}^2/\text{km}$, the transmission

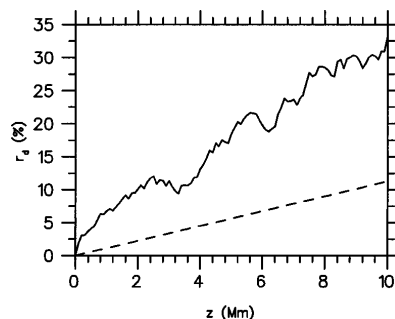


Fig. 2. Energy-depletion ratio along the fiber for the case shown in Fig. 1 (solid curve). The dashed line represents the ratio of the accumulated noise energy and initial soliton energy in the absence of Kerr nonlinearity.

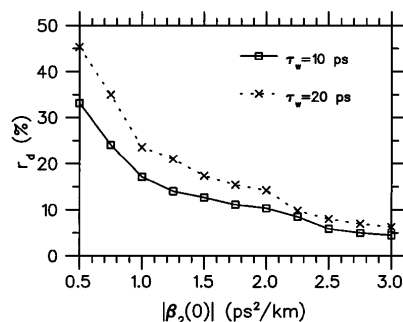


Fig. 3. Energy-depletion ratio r_d versus initial fiber dispersion $|\beta_2(0)|$ for both 10- and 20-ps solitons at a 10,000-km transmission distance.

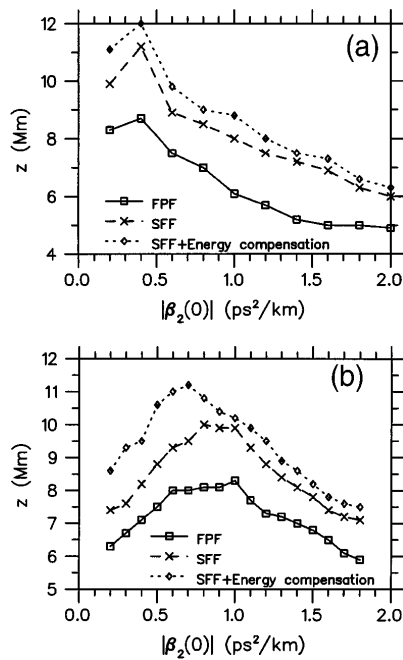


Fig. 4. Allowed transmission distance versus initial fiber dispersion $|\beta_2(0)|$ for (a) 10-ps and (b) 20-ps solitons.

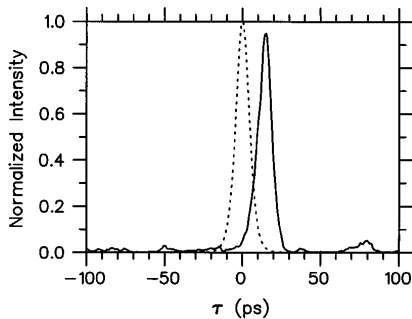


Fig. 5. Soliton pulse shape for the same case as in Fig. 1 (solid curve), except that the energy depletion is completely compensated for. Dotted curve, input soliton pulse shape.

distance is longer for the 10-ps pulse width; for $|\beta_2(0)| > 0.6 \text{ ps}^2/\text{km}$, the transmission distance is longer with the 20-ps pulse width. Although the energy-depletion ratio decreases with pulse width for the same $|\beta_2(0)|$ as shown in Fig. 3, the noise-induced timing jitter is enhanced for the soliton with the shorter pulse width. The transmission distance with the shorter pulse width is less than that with the longer pulse width when $|\beta_2(0)|$ is large.

To compensate for the energy depletion, we can increase amplifier gain to maintain the estimated average soliton energy, $\bar{E}_s = r_c E_{s0}$, where r_c is the energy-

compensation ratio. As the energy depletion increases with distance owing to greater noise power, the required amplifier gain also increases with distance. Figure 5 shows the pulse shape of the soliton for the same case as in Fig. 1, except that the energy depletion is compensated for and $r_c = 1.0$. One can see that the pulse shape is much better than that without the compensation for the energy depletion. However, $r_c = 1.0$ may not be the optimal choice because the generated noise power through soliton-noise FWM increases with r_c . With the energy-compensation ratio r_c adjusted, the maximum transmission distances for different $|\beta_2(0)|$ when sliding filters are used are shown in Fig. 4 by the diamonds. For example, the optimal r_c for the case with a 10-ps soliton are 0.95, 0.8, and 0.5 for $|\beta_2(0)| = 0.2 \text{ ps}^2/\text{km}$, $|\beta_2(0)| = 1.0 \text{ ps}^2/\text{km}$, and $|\beta_2(0)| = 2.0 \text{ ps}^2/\text{km}$, respectively. Comparing the cases without and with energy compensation shown in Fig. 4, we see that the transmission distance can be improved significantly when $|\beta_2(0)|$ is not too large. When $|\beta_2(0)|$ is large, although the soliton pulse width is maintained better with energy compensation, the dispersive wave is larger owing to the greater noise power, where part of the noise is converted from solitons through soliton-noise FWM. The enhancement of soliton-soliton interaction by the dispersive wave increases with $|\beta_2(0)|$.

In conclusion, we have shown the FWM between soliton and amplifier noise in a system with large amplifier spacing, in which DEDF is used as transmission fiber. When a low-dispersion DEDF is used in such a system, the depletion of soliton energy owing to the soliton-noise FWM is significant because of the phase matching. On the other hand, when the higher-dispersion DEDF is used, the FWM is reduced, but the noise-induced timing jitter and soliton-soliton interaction increase. Therefore there exists an optimum fiber dispersion for the maximum transmission distance. The improvement of the soliton system by use of a SFF and compensation for depleted soliton energy were also shown.

This study was partially supported by the National Science Council, Republic of China, under contract NSC 86-2811-E009-002R.

References

1. L. F. Mollenauer, J. P. Gordon, and M. N. Islam, *IEEE J. Quantum Electron.* **QE-22**, 157 (1986).
2. J. P. Gordon and H. A. Haus, *Opt. Lett.* **11**, 665 (1986).
3. K. Tajima, *Opt. Lett.* **12**, 54 (1987).
4. A. Mecozzi, J. D. Moores, H. A. Haus, and Y. Lai, *Opt. Lett.* **16**, 1841 (1991).
5. L. F. Mollenauer, J. P. Gordon, and S. G. Evangelides, *Opt. Lett.* **17**, 1575 (1992).